Resveratrol Attenuates High-Fat Diet Induced Hepatic Lipid Homeostasis Disorder and Decreases m6A RNA Methylation

Jiamin Wu
Nanjing Agricultural University
Yi Li
Nanjing Agricultural University
Jiayao Yu
Nanjing Agricultural University
Zhending Gan
Nanjing Agricultural University
wenyao Wei
Nanjing Agricultural University
Chao Wang
Nanjing Agricultural University
Lili Zhang
Nanjing Agricultural University
Tian Wang
Nanjing Agricultural University
xiang zhong (zhongxiang@njau.edu.cn)
Nanjing Agricultural University https://orcid.org/0000-0002-8622-8078

Research

Keywords: Resveratrol, Obesity, Lipid metabolism, M6A RNA methylation

Posted Date: May 21st, 2020

DOI: https://doi.org/10.21203/rs.3.rs-29620/v1

Abstract

Purpose: *N* ^{6}-methyladenosine (m^6A) mRNA methylation is affected by dietary factors and associated with lipid metabolism, however, whether the regulatory role of resveratrol in lipid metabolism is involved in m^6A mRNA methylation remain unknown. Here, the objective of this study was to investigate the effect of resveratrol on hepatic lipid metabolism and m^6A RNA methylation in the liver of mice.

Methods: A total of 24 male mice were randomly allocated to LFD (low-fat diet), LFDR (low-fat diet + resveratrol), HFD (high-fat diet), and HFDR (high-fat diet + resveratrol) groups for 12 weeks (n = 6/group).

Results: Compared to the HFD group, dietary resveratrol supplementation reduced the body weight, relative abdominal, epididymal, and perirhemtric fat weight, however, significantly increased average daily feed intake in mice given high-fat diet. The amounts of serum low density lipoprotein cholesterol (LDL), liver total cholesterol (TC), triacylglycerol (TAG) were significantly decreased by resveratrol supplementation. In addition, Resveratrol significantly enhanced the levels of peroxisome proliferator-activated receptor alpha (*PPARα*), peroxisome proliferator-activated receptor beta/delta (*PPARβ/δ*), cytochrome P450 family 4 subfamily a polypeptide 10/14 (*CYP4A10/14*), acyl-CoA oxidase 1 (*ACOX1*), and fatty acid-binding protein 4 (*FABP4*) mRNA, and inhibited acyl-CoA carboxylase (*ACC*) mRNA levels in the liver. Furthermore, the resveratrol in high-fat diet increased the transcript levels of methyltransferase like 3 (*METTL3*), alkB homolog 5 (*ALKBH5*), fat mass and obesity associated protein (*FTO*), and YTH domain family 2 (*YTHDF2*), whereas decreased the level of YTH domain family 3 (*YTHDF3*) and m^6A abundance in mice liver.

Conclusion: The beneficial effect of resveratrol on lipid metabolism disorder under high-fat diet may be due to decrease of m^6A RNA methylation and increase of *PPARα* mRNA, providing mechanistic insights into the function of resveratrol in alleviating the disturbance of lipid metabolism in mice.

Introduction

Lipids are critical nutrients and energy substances in both human and animals, whereas long-term high-fat diet could result in defective nutritional metabolism, particularly in hepatic lipid metabolism [1]. Hepatic lipid metabolic disorder contributes to the development of obesity, which is involved in many serious chronic diseases, including diabetes, hypertension, and even cancer [2]. Therefore, further developing the effective investigation in the regulation of hepatic lipid metabolism is necessary and could offer potential theory to prevent and treat metabolic diseases.

Resveratrol (3, 5, 4'-trihydroxystilbene) is a natural polyphenolic compound found in plants. It is well known that resveratrol has antioxidative [3, 4], anti-inflammatory [5, 6], anticarcinogenic [7, 8], antibacterial [9, 10] effects and exhibits protective nature in the regulation of liver injury [11] Furthermore, accumulating evidences reported that resveratrol participates in attenuating abnormal lipid metabolism. Ran et al. [12] found that the regulatory roles of resveratrol in lipid metabolism balance of zebrafish under dietary stress conditions are associated with the AMP-activated protein kinase alpha (AMPKα) pathway. Resveratrol also improves serum lipid characters and reverses body fat deposition in a pig model [13]. Sun et al. [14] suggested that resveratrol could restore clock-mediated dysfunctional lipid metabolism in high-fat-fed mice via the activation of clock machinery. However, the potential molecular network of resveratrol in regulating lipid metabolism is unclear.

N^6-methyladenosine (m^6A) is the most abundant mRNA modification in eukaryotes, which accounts for over sixty percent of all RNA chemical modifications [15]. M^6A modification can be dynamically installed, erased and recognized by the m^6A methyltransferase complex (METTL3, METTL14, and WTAP) [16–18], demethylases (FTO and ALKBH5)

[19, 20], and m^6A binding proteins (YTHDF1, YTHDF2, YTHDF3) [21–23]. M^6A RNA methylation has received great attention due to its function on cellular processes, including mRNA splicing, export, localization, translation, stability, and translation efficiency [16, 22–24]. In addition, m^6A modification also plays a key role in biological processes such as cellular differentiation, lipid accumulation, and energy metabolism [25–27]. Recently, dietary factors have been used to regulate m^6A RNA methylation, such as betaine [28, 29] and curcumin [30]. Li et al. [31] showed that maternal high fat exposure led to imbalanced m^6A mRNA modification in offspring. However, the effect of resveratrol on m^6A modification is unknown.

We speculated that resveratrol in a high-fat diet alleviated liver lipid metabolism disorders may be due to the changes of m^6A levels. Thus, the aim of this study was to investigate the effect of resveratrol on lipid metabolism and m^6A RNA methylation in the liver of mice.

Materials And Methods

Animal and Diets

All experimental procedures were conducted in conformity with the Chinese Guidelines for Animal Welfare, and were approved by the Animal Care Advisory Committee of Nanjing Agricultural University, China (NJAU-CAST-2015-095). Twenty-four C57BL/6J male mice (5 weeks of age) were from Yangzhou Institute of Experimental Animals (SCXK (Su) 2012-0004). After three weeks of acclimation, mice were randomly distributed into four groups of 6 mice each as follows: 10% low-fat diet (LFD), 10% low-fat diet and dietary supplemented with 276 mg/kg of resveratrol (LFDR), 60% high-fat diet (HFD), 60% high-fat diet and dietary supplemented with 400 mg/kg of resveratrol (HFDR) [14, 32, 33]. There are 400 mg of resveratrol per kilogram of high-fat diet, and the caloric value was about 5.2 kcal/g, while that of low-fat diet was 3.6 kcal/g. In order to balance the amount of resveratrol per unit of energy between LFDR and HFDR diets, the amount of resveratrol per kilogram of low-fat diet was 276 mg. During the entire 12-week experiment, all mice were housed at 22 ± 1 °C under a 12-h light cycle and were allowed to drink and feed ad libitum. In addition, body weight and food consumption were recorded weekly.

Resveratrol (CAS: 501-36-0, purity over 99%) used in the experiment was bought from Sigma-Aldrich. We used HPLC analysis to confirm the concentration of resveratrol. All diets were manufactured by Trophic Animal Feed Co., Ltd. (Nantong, China). Composition and nutritional levels of mice diet based on AIN93 [34]. The LFD group was fed a TP 2330055MC diet consisting of casein, starch, dextrin, sucrose, soybean oil, mineral mixtures, vitamin mixtures, cystine, choline, and TBHQ. The HFD group was fed a TP 2330055M diet consisting of casein, starch, sucrose, lard, mineral mixtures, vitamin mixtures, cystine, choline, and TBHQ. The LFD consist of 10% fat, 14% protein and 76% carbohydrate, and HFD consist of 60% fat, 14% protein and 26% carbohydrate.

Sample Collection

Mice body weight in the HFD group was higher up to 4 g (> 4 g) than in the LFD group at the end of 12 weeks, suggesting that we successfully built a model of obesity [35]. Blood samples were collected by cardiac puncture technique following anesthesia with carbon dioxide, centrifuged at 3500 r/min for 10 min at 4 °C, and then stored at −80 °C for the further determination. The liver was quickly removed, weighed, and thoroughly washed with PBS. A portion of the liver was stored separately in 10% buffered formalin solution for histopathological examination. The rest of liver was snap frozen using liquid nitrogen for further investigation.

Biochemical Parameters Analysis

The liver sample (0.2 g) from − 80 °C was suspended in ice-cold physiological saline (1.8 mL, 7.5 g/L NaCl diluent) and then homogenized at 13500 g for one minute in ice-bath using homogenizer (Tekmar, Ohio, USA). The homogenate was spun at 3000 g for 15 min at a temperature of 4 °C, and the supernatant was collected and analyzed immediately.

The levels of total cholesterol (TC, CAS: A111-1-1), triacylglycerol (TAG, CAS: A110-1-1), and low density lipoprotein cholesterol (LDL, CAS: A113-1-1) were measured using commercial kits (Nanjing Jiancheng Bioengineering Institute, Jiangsu, China) by a Microplate Reader (Thermo Scientific, Wilmington, DE, USA) with a detection wavelength of 510 nm, 510 nm, and 546 nm, respectively. All experimental procedures were performed according to the manufacturer's protocols. All hepatic measurements were normalized to concentrations of total protein for inter-sample comparisons.

Hematoxylin-eosin Staining

The liver sections fixed in 10% paraformaldehyde were dehydrated with graded dilutions of ethanol, and embedded in paraffin. Then tissues (5 μm) were deparaffinized with xylene and rehydrated with graded dilutions of ethanol. The slides were stained with hematoxylin and eosin (H & E). A light microscope (Nikon ECLIPSE 80i, Nikon Corporation) was used to photograph and evaluate the pathological changes.

Oil-red Staining

For oil-red staining, fresh livers frozen at -80 °C were sectioned (5 μm thick), fixed in a slide, and dissolved in propylene glycol (2 minute). Slides were transferred to oil-red O solution (Sigma, Steindorf, Germany, CAS: O1516) for 1 hours, then immersed in 85% propylene glycol (1 min), washed two times in water. Finally, slides were counterstained in hematoxylin solution (10 s), and mounted using glycerin.

Rna Extraction And Qrt-pcr

Total RNA of snap-frozen liver was extracted using TRIZol reagent (TaKaRa, Otsu, Shiga, Japan, CAS: 9108). The RNA integrity was examined on one percent of agarose gel using GelRed staining. The RNA contents were quantified by Thermo NanoDrop 2000 Ultra Trace Visible Spectrophotometer (Thermo Fisher, Waltham, MA, USA). After that, 1000 ng total RNA was reverse-transcribed into cDNA in a 20 μl reaction volume using the PrimerScript RT Reagent kit (TaKaRa, Otsu, Shiga, Japan, CAS: RR036A). Real-time PCR was performed on the QuantStudioTM Design & Analysis Software (Thermo Fisher, Waltham, MA, USA). Primers were synthesized by Invitrogen Biotech Co. Ltd. (Shanghai, China) and listed in Table 1. qRT-PCR was performed in a 20 μl reaction mixture using ChamQ Universal SYBR qPCR 1Master Mix (Vazyme Biotech Co.,Ltd, Nanjing, China, CAS: Q311-02). The thermal profile was 3 min at 95 °C, 10 sec at 95 °C for 40 cycles, then 30 sec at 60 °C. The relative gene expression was calculated based on the $2^{-\Delta\Delta CT}$ method after normalization to housekeeping gene GAPDH. Samples in the LFD group were used as calibrator.

Table 1
Primers used for qRT-PCR

Genes	Forward	Reverse
GAPDH	GGCAAATTCAACGGCACAGT	AGATGGTGATGGGCTTCCC
ACC	GCCTCCGTCAGCTCAGATAC	ATGTGAAAGGCCAAACCATC
FABP4	CTTTGCCACAAGGAAAGTGG	TCCCCATTTACGCTGATGAT
FATP4	ACTGTTCTCCAAGCTAGTGCT	GATGAAGACCCGGATGAAACG
SREBP-1c	GGAGCCATGGATTGCACATT	GGCCCGGGAAGTCACTGT
PPaRγ	CTGACAGGACTGTGTGAC	TCTGTGTCAACCATGGTAAT
PPaRα	TGCAAACTTGGACTTGAACG	AGGAGGACAGCATCGTGAAG
CYP4A10	AGGTGTGGCCAAATCCAGAG	AATGCAGTTCCTGGCTCCTC
CYP4A14	ACCCTCCAGCATTTCCCATG	CTGTAAGCAGGCACTTGGGA
ACOX1	CTGGTGGGTGGTATGGTGTC	AATCTGGCTGCACGTAGCTT
CPT1α	GTGAAAAGCACCAGCACCTG	GAAAGGTGAGTCGACTGCCA
PPARβ/δ	CCTCCATCGTCAACAAAGACG	TTTAGCCACTGCATCATCTGGGCATGCTC
METTL3	AGCAGAGCAAGAGACGAATTATC	GGTGGAAAGAGTCGATCAGCA
METTL14	AGAGAAACCTGCAGGGCTTC	TCCTCCTGCTGCATTTCCAG
FTO	TTCATGCTGGATGACCTCAATG	GCCAACTGACAGCGTTCTAAG
ALKBH5	CGCGGTCATCAACGACTACC	ATGGGCTTGAACTGGAACTTG
YTHDF1	ATGCCCAACCTACTTCTGCC	GAACACCCGCCCACTCTTAA
YTHDF2	GAGCAGAGACCAAAAGGTCAAG	CTGTGGGCTCAAGTAAGGTTC
YTHDF3	ATGCCCAACCTACTTCTGCC	GAACACCCGCCCACTCTTAA

[a] *GAPDH*, Glyceraldehyde-3-phosphate dehydrogenase; *ACC*, Acyl-CoA carboxylase; *FABP4*, Fatty acid-binding protein 4; *FATP4*, Fatty acid transporter protein 4; *SREBP-1c*, Sterol regulatory element binding protein-1c; *PPARα*, Peroxisome proliferator-activated receptor alpha; *PPARγ*, Peroxisome proliferator-activated receptor gamma; *CYP4A10*, Cytochrome P450 family 4 subfamily a polypeptide 10; *CYP4A14*, Cytochrome P450 family 4 subfamily a polypeptide 14; *ACOX1*, Acyl-CoA oxidase 1; *CPT1α*, Carnitine palmitoyltransferase 1 alpha; *PPARβ/δ*, Peroxisome proliferator-activated receptor beta/delta; *METTL3*, Methyltransferase like 3; *METTL14*, Methyltransferase like 14; *FTO*, Fat mass and obesity associated; *ALKBH5*, alkB homolog 5; *YTHDF1*, YTH domain family 1; *YTHDF2*, YTH domain family 2; *YTHDF3*, YTH domain family

Measurement Of Total Ma

A total of 200 ng aliquots of mRNA was extracted from liver. EpiQuikTM m^6A RNA Methylation Quantification Kit was used to detect total RNA m^6A levels (Epigentek, Wuhan, China, CAT. No. p-9005) according to our previous studies [36–38]. Briefly, m^6A on RNA was captured using m^6A antibodies after binding to strip wells using binding solution. The signal of m^6A was quantified colorimetrically via reading the absorbance on a microplate reader at 450 nm (Thermo Fisher, Waltham, MA, USA). The m^6A level was calculated by OD intensity.

Western Blot

Proteins from each 20 mg liver were extracted using tissue lysis buffer (Beyotime Biotechnology, Shanghai, China, CAS: P0013B) at a temperature of 4 °C. Then, the homogenate was centrifuged at 12000 g and 4 °C for 30 min. The protein concentrations were measured using a commercial kit (Beyotime Biotechnology, Shanghai, China, CAS: P0012). Samples (40 μg of protein) were mixed with 5 × sample buffer and boiled at one hundred degrees centigrade for 10 min. Separation of the protein samples were performed on 10% SDS-PAGE gels and electrotransferred onto an immobile membrane (PVDF membrane, Merck Millipore, Darmstadt, Germany, CAS: IPVH00010) with transfer buffer. The PVDF membranes were incubated overnight with primary antibody at a temperature of 4 °C after block of five percent of non-fat dry milk diluted in TBST for 1 hours at RT. After 3 times washing, horseradish peroxidase-conjugated secondary antibodies (1:7500, Abcam, ab205718 or ab205719) were applied to incubation of the membranes for 90 min at RT. The bands were visualized using the ECL detection kit (ECL-plus, Beyotime Biotechnology, Shanghai, China, CAS: P0018S). The images were analyzed by a luminescence image analyzer LAS-4000 system (Fujifilm Co. Ltd., Tokyo, Japan) and were quantified by Gel-Pro Analyzer 4.0 software (Media Cybernetics, Silver Spring MD, USA). Some information about primary antibodies as follows: methyltransferase like 3 (1:2000, METTL3, Abcam, ab240595), YTH domain family 2 (1:2000, YTHDF2, Proteintech, 24744-1-AP), alkB homolog 5 (1:1500, ALKBH5, Proteintech, 16837-1-AP), FTO (1:1500 Proteintech, 27226-1-AP), and β-actin (1:10000, Proteintech, 60008-1-Ig).

Statistical Analysis

Data were analyzed by the two-way ANOVA and were present as means ± SD (standard deviations) after confirming normally distributed patterns. The classification variables were dietary resveratrol supplementation (LFD + HFD × LFDR + HFDR), high-fat diet (LFD + LFDR × HFD + HFDR), and their interaction (LFD × LFDR × HFD × HFDR). The significant difference among groups was examined by Duncan's multiple range tests when significant difference of resveratrol × high-fat diet interaction was examined. The SPSS 21.0 statistical software (SPSS, Inc., Chicago, IL, USA) was used to analyze the present results. P-values less than 0.05 were considered as statistically significant level. P-values less than 0.01 were regarded as very significant.

Results

Effect of resveratrol on weight gain and feed intake

During the entire 12-week period, mice body weight in the HFD group was higher than that of the HFDR group (Figure. 1a). The final body weight in mice fed LFD showed was significantly (32.87%) lower than mice in high-fat diet exposure ($P < 0.05$, Figure. 1a). We also found that resveratrol in a high-fat diet significantly reduced the average daily gain in mice compared to the HFD group ($P < 0.05$, Figure. 1d). Besides, the addition of resveratrol in high-fat or low-fat diet significantly increased the average daily feed intake ($P < 0.05$, Figure. 1e and 1f).

Effect Of Resveratrol On Liver Weight And Fat Mass

Mice given high-fat diet (HFD and HFDR) exhibited significant increase of the liver, abdominal, epididymal, and perirhemtric fat weight ($P < 0.05$, Figure. 2a, 2c and 2e) relative to mice fed LFD (LFD and LFDR). Resveratrol significantly decreased the weight of abdominal and epididymal fat in the high-fat diet compared to HFD group ($P < 0.05$, Figure. 2c). Meanwhile, the addition of resveratrol in the high-fat diet significantly increased relative liver weight

of HFDR mice ($P < 0.05$) and decreased relative abdominal, epididymal and perirhemtric fat weight compared to HFD group ($P < 0.05$, Figure. 2b, 2d and 2f).

Hepatic Morphology And Lipid Accumulation

Hepatic morphology and lipid accumulation were showed in Figure. 3. Extensive macrocytic steatosis around the peripheral sinus region and fatty degeneration of microvesicles were observed in HFD mice. The steatosis and ballooning degeneration decreased by the addition of resveratrol in HFDR mice (Figure. 3a). Further oil-red O staining analysis of those mice revealed the more appearance of lipid droplets within HFD group (Figure. 3b). Moreover, treatment of resveratrol for 12 weeks decreased hepatic intracellular lipid droplets in HFDR mice.

Lipid Metabolic Index

The contents of TC and LDL in the serum of HFD mice were significantly higher than those of LFD mice ($P < 0.05$, Table 2). The level of LDL was lower ($P < 0.05$) in serum of HFDR mice ($P < 0.05$) than HFD mice. However, the differences in TAG and TC in serum were not found between the HFD and HFDR groups. In addition, there was a significant enhancement ($P < 0.05$) in the concentrations of TAG, TC, and LDL in the liver of HFD mice compared with mice fed LFD alone. Notably, resveratrol could reverse the increase of TAG induced by high-fat diet ($P < 0.05$).

Table 2
Effects of resveratrol on high-fat diet-induced on the lipid levels in mice.

	LFD		**LFDR**		**HFD**		**HFDR**		***P*-value**		
Items	Mean	SD	Mean	SD	Mean	SD	Mean	SD	HFD	RES	HFD × RES
Serum											
TAG (mmol/L)	1.08	0.24	1.01	0.17	1.13	0.16	1.11	0.09	0.105	0.758	0.554
TC (mmol/L)	3.19^{c}	0.36	3.69^{bc}	0.43	4.40b^{a}	0.42	4.28^{ab}	0.83	0.001	0.410	0.173
LDL (mmol/L)	0.32^{b}	0.06	0.33^{b}	0.11	0.54^{a}	0.29	0.35^{b}	0.06	0.006	0.038	0.016
Liver											
TAG (mmol/gprot)	0.57^{b}	0.07	0.65^{b}	0.065	1.20^{a}	0.122	0.70^{b}	0.089	< 0.001	0.012	0.001
TC (mmol/gprot)	2.40^{b}	0.66	2.38^{b}	0.47	3.44^{a}	0.99	2.51^{b}	0.41	0.046	0.130	0.152
LDL (mmol/gprot)	2.42^{c}	0.53	2.84^{bc}	0.60	4.23^{a}	0.90	3.64^{ab}	1.19	0.001	0.809	0.157

[a] TC, total cholesterol; TAG, triacylglycerol; LDL, low-density lipoprotein.

[b] Different or the same superscript letters demonstrate statistically significant differences ($P < 0.05$) and no differences ($P > 0.05$) in groups, respectively (n = 6). LFD, LFDR, HFD, and HFDR represent low-fat, low-fat + 0.0276% resveratrol, high-fat, and high-fat + 0.04% resveratrol, respectively.

Lipid Metabolism Associated Messenger Rna Expression

We next measured the expression of lipid metabolism regulatory genes. Compared with LFD mice, high-fat diet downregulated the expression of hepatic *PPARα* mRNA, upregulated the abundances of *ACC*, *SREBP-1c*, and *PPARγ* mRNA in the liver ($P < 0.05$, Figure. 4). Dietary resveratrol supplementation in the high-fat diet increased the expression of hepatic *PPARα*, *PPARβ/δ*, *CYP4A10, CYP4A14, ACOX1*, *FATP4*, and *FABP4* mRNA compared to mice given a HFD diet ($P < 0.05$). However, the levels of *ACC* and *PPARγ* mRNA in HFDR mice were reduced by resveratrol compared to untreated HFD group ($P < 0.05$). We also noted that dietary resveratrol in the low-fat diet increased ($P < 0.05$) the expression of *PPARα*, *PPARβ/δ*, *CPT1α, CYP4A10, CYP4A14, ACOX1*, and *FATP4* mRNA relative to LFD.

Effects Of Resveratrol On Ma Rna Methylation

To investigate the regulation of resveratrol on mRNA m^6A methylation, we tested m^6A and m^6A-related genes and proteins. Compared with LFD mice, high-fat diet significantly downregulated the gene expression of *ALKBH5* and *FTO* while obviously increased the level of *YTHDF3* ($P < 0.05$, Figure. 5a). Moreover, resveratrol significantly elevated ($P < 0.05$) the levels of *METTL3*, *YTHDF2*, *FTO* and *ALKBH5* mRNA and decreased the mRNA expression of *YTHDF3* in HFDR mice ($P < 0.05$, Figure. 5a). The results demonstrated that resveratrol significantly enhanced YTHDF2 protein ($P < 0.05$, Figure. 5b). In addition, high-fat dietary resveratrol supplementation decreased the content of m^6A (Figure. 5c).

Discussion

Growing evidences uncover the protective potential of resveratrol in regulating lipid metabolism, however, its mechanism at the post-transcriptional level is still incompletely known. In this study, we noted that dietary resveratrol supplementation alleviated lipid disorders induced by high-fat diets and decreased m^6A RNA methylation in the liver of mice. The present results suggest that the beneficial role of resveratrol in lipid metabolism may be involved in the modification of m^6A RNA methylation.

PPARα, a molecular target of resveratrol [39], participates in the promotion of adipocyte differentiation, the modulation of nutritional metabolism, and the inhibition of inflammatory response [40, 41]. Previous study showed that resveratrol increased the levels of sirtuin-1 (SIRT1) and PPARα to mediate its protective effect on hypertension under maternal high-fat diet in the kidneys of male progeny [42]. In addition, resveratrol enhanced hepatitis B virus transcription and replication followed by increase of transcriptional activity of PPARα in HepG2 cells and rats [43]. Here, hepatic elevation of *PPARα* mRNA was found in mice given resveratrol, which together with the PPARα-dependent enhancement in expression of PPARα marker genes, including *CYP4A10, CYP4A14*, and *ACOX1*. So far, activation of PPARα transcription plays crucial roles in the regulation of resveratrol on lipid metabolism. Interestingly, growing investigations exhibited the interaction of PPARα with adipocyte-fatty acid binding protein (A-FABP, FABP4), a late adipocyte differentiation marker. Boiteux et al. firstly found the positive correlation between FABP4 and PPARα in urothelial cancer cells [44]. Lu et al. also showed that increase of FABP4 expression was observed after activation of PPARα [45]. The current study noted that resveratrol significantly increased the mRNA expression of *PPARα* and *FABP4* in high-fat-fed mice. Thus, we speculated that resveratrol-mediated PPARα activation regulated hepatic lipid metabolism by increasing the expression of FABP4. However, its potential mechanism at the epitranscriptomic level is not sufficiently known.

M^6A takes place at transcriptional levels of nitrogen or oxygen atoms from S-adenosylmethionine (SAM) as a methyldonor [46]. M^6A can regulate mRNA splicing, export, localization, translation and stability, thus it participates in

the modulation of gene expression [47, 48]. Recent studies revealed that m^6A modification plays a critical role in lipid metabolism. Liu et al [16] indicated that silence of METTL3 reduced the abundance of m^6A and increased the transcriptional activity of PPARα in HeLa cells. Furthermore, our previous study discovered that reduction of m^6A modification via silence of METTL3 or YTHDF2 up-regulated the lifetime and expression of PPARα and affected the mRNA m^6A methylation of PPARα, and eventually reversed lipid accumulation [49]. Interestingly, it is worth noting that some dietary factors are sensitive to m^6A methylation and metabolic regulation. Li et al. [31] found that maternal high-fat diet changes mRNA m^6A modification and its regulatory genes in offspring. In addition, cycloleucine (methylation inhibitor) and betaine (methyl donor) oppositely modulate m^6A levels and lipid deposition [50]. Our previous data also indicated that dietary curcumin or resveratrol supplementation changed the hepatic m^6A abundance in piglets [30, 51]. Here, we observed that resveratrol decreased the hepatic lipid accumulation together with elevation mRNA levels of m^6A methylases and demethylases, increase of YTHDF2 expression, and obvious reduction of *YTHDF3* mRNA expression and hepatic m^6A level in high-fat-treated mice. Thus, these observations, in part, suggested that the regulation of resveratrol on the transcriptional PPARα activity may be associated with the modification of m^6A RNA methylation. Further investigation is required to explore the precise mechanism of resveratrol on m^6A RNA methylation.

Conclusions

Resveratrol attenuated high-fat diet induced abnormal lipid metabolism and affected m^6A profiles in the liver of mice. The alleviating effect of resveratrol on disorder of lipid metabolism under high-fat diet may be associated with the decrease of m^6A methylation and increase of *PPARα* mRNA. The present work offers insights into the underlying avenues for the treatment of some relevant liver diseases.

Abbreviations

m^6A, N^6-methyladenosine; GAPDH, Glyceraldehyde-3-phosphate dehydrogenase; ACC, Acyl-CoA carboxylase; FABP4, Fatty acid-binding protein 4; FATP4, Fatty acid transporter protein 4; SREBP-1c, Sterol regulatory element binding protein-1c; PPARα, Peroxisome proliferator-activated receptor alpha; PPARγ, Peroxisome proliferator-activated receptor gamma; CYP4A10, Cytochrome P450 family 4 subfamily a polypeptide 10; CYP4A14, Cytochrome P450 family 4 subfamily a polypeptide 14; ACOX1, Acyl-CoA oxidase 1; CPT1α, Carnitine palmitoyltransferase 1 alpha; PPARβ/δ, Peroxisome proliferator-activated receptor beta/delta; METTL3, Methyltransferase like 3; METTL14, Methyltransferase like 14; FTO, Fat mass and obesity associated; ALKBH5, alkB homolog 5; YTHDF1, YTH domain family 1; YTHDF2, YTH domain family 2; YTHDF3, YTH domain family 3; TC, Total cholesterol; TAG, triacylglycerol; LDL, low-density lipoprotein. AMPKα, AMP-activated protein kinase alpha; SIRT1, sirtuin-1; SAM, S-adenosylmethionine

Declarations

Declarations

Ethics approval and consent to participate

All experimental procedures were conducted in conformity with the Chinese Guidelines for Animal Welfare, and were approved by the Animal Care Advisory Committee of Nanjing Agricultural University, China (NJAU-CAST-2015-095).

Consent for publication

Not applicable.

Availability of data and materials

Data sharing is not applicable to this article as no datasets were generated or analyzed during the current study.

Competing interests

The authors declare that they have no conflict of interest.

Funding

The study was supported by the grants from National Natural Science Foundation of China (NO. 31872391).

Authors' contributions

Jiamin Wu, Yi Li, Xiang Zhong designed the research. Jiamin Wu, Yi Li, Xiang Zhong wrote the paper, and Jiamin Wu was a major contributor in writing the manuscript. Jiamin Wu, Yi Li, Zhending Gan searched and read the literature. Jiamin Wu, Yi Li, Wenyao Wei, Jiayao Yu performed experiments. Chao Wang, Lili Zhang, Tian Wang provided essential suggestion and revision. Xiang Zhong had primary responsibility for final content. All authors read and approved the final manuscript.

Acknowledgements

Not applicable.

References

1. Feltenberger J, Andrade J, Paraíso A, Barros L, Filho A, Sinisterra R, De Sousa F, Paula A, Campagnole-Santos M, Qureshi M, et al. Oral Formulation of Angiotensin-(1–7) Improves Lipid Metabolism and Prevents High-Fat Diet-Induced Hepatic Steatosis and Inflammation in Mice. Hypertension. 2013;62:324–30.
2. Tessari P, Coracina A, Cosma A, Tiengo A. Hepatic lipid metabolism and non-alcoholic fatty liver disease. Nutr Metab Cardiovasc Dis. 2009;19:291–302.
3. Fu S, Lv R, Wang L, et al. Resvervatol, a antioxidant protects spinal cord injury in rats by suppressing MAPK pathway. Saudi J Biol Sci. 2018;25:259–66.
4. Truong VL, Jun M, Jeong WS. Role of resveratrol in regulation of cellular defense systems against oxidative stress. Biofactors. 2018;44:36–49.
5. Xu M, Cheng Z, Ding Z, et al. Resveratrol enhances IL-4 receptor-mediated anti-inflammatory effects in spinal cord and attenuates neuropathic pain following sciatic nerve injury. Mol Pain. 2018;14:2070395971.
6. Zhou ZX, Mou SF, Chen XQ, Gong LL, Ge WS. Anti-inflammatory activity of resveratrol prevents inflammation by inhibiting NF–κB in animal models of acute pharyngitis. Mol Med Rep. 2018;17:1269–74.
7. Zheng X, Jia B, Song X, et al. Preventive Potential of Resveratrol in Carcinogen-Induced Rat Thyroid Tumorigenesis. Nutrients. 2018;10:e279.
8. Kisková T, Jendželovský R, Rentsen E, et al. Resveratrol enhances the chemopreventive effect of celecoxib in chemically induced breast cancer in rats. Eur J Cancer Prev. 2014;23:506–13.
9. Kukric' ZZ, Trivunovi NL. T. Antibacterial activity of cis- and trans-resveratrol isolated from Polygonum cuspidatum rhizome. Acta Periodica Technologica. 2006;37:131–6.

10. Duarte A, Alves AC, Ferreira S, Silva F, Domingues FC. Resveratrol inclusion complexes: Antibacterial and anti-biofilm activity against Campylobacter spp. and Arcobacter butzleri. Food Res Int. 2015;77:244–50.
11. Ajmo J, Liang X, Rogers C, Pennock B, You M. Resveratrol Alleviates Alcoholic Fatty Liver in Mice. Am J Physiol Gastrointest Liver Physiol. 2008;295:G833–42.
12. Ran G, Ying L, Li L, et al. Resveratrol ameliorates diet-induced dysregulation of lipid metabolism in zebrafish (Danio rerio). Plos One. 2017;12:e180865.
13. Zhang C, Luo J, Yu B, Chen J, Chen D. Effects of resveratrol on lipid metabolism in muscle and adipose tissues: A reevaluation in a pig model. J Funct Foods. 2015;14:590–5.
14. Sun LJ, Wang Y, Song Y, Cheng XR, Xia SF, Rahman M, Shi YH. Le G W. Resveratrol restores the circadian rhythmic disorder of lipid metabolism induced by high-fat diet in mice. Biochem Bioph Res Co. 2015;458:86–91.
15. Wei CM, Gershowitz A, Moss B. Methylated nucleotides block 5' terminus of HeLa cell messenger RNA. Cell. 1975;4:379–86.
16. Liu J, Yue Y, Han D, et al. A METTL3–METTL14 complex mediates mammalian nuclear RNA N6-adenosine methylation. Nat Chem Biol. 2014;10:93–5.
17. Ping XL, Sun BF, Wang L, et al. Mammalian WTAP is a regulatory subunit of the RNA N6-methyladenosine methyltransferase. Cell Res. 2014;24:177–89.
18. Wang X, Feng J, Yuan X, et al. Structural basis of N6-adenosine methylation by the METTL3–METTL14 complex. Nature. 2017;542:575–8.
19. G J, Y F, X Z, et al. N6-methyladenosine in nuclear RNA is a major substrate of the obesity-associated FTO. Nat Chem Biol. 2011; 7: 885–887.
20. Zheng G, Dahl JA, Niu Y, et al. ALKBH5 is a mammalian RNA demethylase that impacts RNA metabolism and mouse fertility. Rna Biol. 2013;49:18–29.
21. Dominissini D, Moshitchmoshkovitz S, Schwartz S, et al. Topology of the human and mouse m6A RNA methylomes revealed by m6A-sEq. Nature. 2012;485:201–6.
22. Wang X, Lu Z, Gomez A, et al. N6-methyladenosine-dependent regulation of messenger RNA stability. Nature. 2014;505:117–20.
23. Liu N, Dai Q, Zheng G, et al. N6-methyladenosine-dependent RNA structural switches regulate RNA-protein interactions. Nature. 2015;518:560–4.
24. Meyer KD, Saletore Y, Zumbo P, et al. Comprehensive analysis of mRNA methylation reveals enrichment in 3' UTRs and near stop codons. Cell. 2012;149:1635–46.
25. Li YW, Toth Y. JI, et al. N6-methyladenosine modification destabilizes developmental regulators in embryonic stem cells. Nat Cell Biol. 2014;16:191–8.
26. Wang X, Zhu L, Chen J, Wang Y. mRNA m6A methylation downregulates adipogenesis in porcine adipocytes. Biochem Biophys Res Commun. 2015;459:201–7.
27. Zhao X, Yang Y, Sun BF, et al. FTO-dependent demethylation of N6-methyladenosine regulates mRNA splicing and is required for adipogenesis. Cell Res. 2014;24:1403–19.
28. Chen J, Zhou X, Wu W, Wang X, Wang Y. FTO-dependent function of N6-methyladenosine is involved in the hepatoprotective effects of betaine on adolescent mice. J Physiol Biochem. 2015;71:405–13.
29. Kang H, Zhang Z, Yu L, et al. FTO reduces mitochondria and promotes hepatic fat accumulation through RNA demethylation. J Cell Biochem. 2018;119:5676–85.
30. Lu N, Li X, Yu J, et al. Curcumin Attenuates Lipopolysaccharide-Induced Hepatic Lipid Metabolism Disorder by Modification of m6A RNA Methylation in Piglets. Lipids. 2018;53:53–63.

31. Li X, Yang J, Zhu Y, et al. Mouse Maternal High-Fat Intake Dynamically Programmed mRNA m6A Modifications in Adipose and Skeletal Muscle Tissues in Offspring. Int J Mol Sci. 2016;17:e1336.
32. Tomayko EJ, Cachia AJ, Chung HR, Wilund KR. Resveratrol supplementation reduces aortic atherosclerosis and calcification and attenuates loss of aerobic capacity in a mouse model of uremia. J Med Food. 2014;17:278–83.
33. Kopec A, Piatkowska E. Effect of resveratrol on selected biochemical parameters in rats fed high fructose diet. Acta Scientiarum Polonorum Technologia Alimentaria. 2013;12:395–402.
34. Reeves PG. Components of the AIN-93 diets as improvements in the AIN-76A diet. J Nutr. 1997;127:838–41.
35. Hariri N, Thibault L. High-fat diet-induced obesity in animal models. Nutr Res Rev. 2010;23:270–99.
36. Zhang S, Zhao BS, Zhou A, et al. m6A Demethylase ALKBH5 Maintains Tumorigenicity of Glioblastoma Stem-like Cells by Sustaining FOXM1 Expression and Cell Proliferation Program. Cancer Cell. 2017;31:591–606.
37. Slobodin B, Han R, Calderone V, et al. Transcription Impacts the Efficiency of mRNA Translation via Co-transcriptional N6-adenosine Methylation. Cell. 2017;169:326–37.
38. Yuen KC, Xu B, Krantz ID, Gerton JL. NIPBL Controls RNA Biogenesis to Prevent Activation of the Stress Kinase PKR. Cell Rep. 2015;14:93–102.
39. Yoshie, Takizawa R, Nakata K, Fukuhara H, Yamashita H, Kubodera H, Inoue. The 4'-hydroxyl group of resveratrol is functionally important for direct activation of PPARα. PloS one. 2015;10:e0120865.
40. Brocker CN, Yue J, Kim D, et al. Hepatocyte-specific PPARA expression exclusively promotes agonist-induced cell proliferation without influence from nonparenchymal cells. Am J Physiol Gastrointest Liver Physiol. 2017;312:283–99.
41. Kang HS, Cho HC, Lee JH, et al. Metformin stimulates IGFBP-2 gene expression through PPARalpha in diabetic states. Sci Rep-Uk. 2016;6:23665.
42. Tain YL, Lin YJ, Sheen JM, et al. Resveratrol prevents the combined maternal plus postweaning high-fat-diets-induced hypertension in male offspring. J Nutr Biochem. 2017;48:120–7.
43. Shi Y, Li Y, Huang C, et al. Resveratrol enhances HBV replication through activating Sirt1-PGC-1α-PPARα pathway. Sci Rep-Uk. 2016;6:24744.
44. Boiteux G, Lascombe I, Roche E, et al. A-FABP, a candidate progression marker of human transitional cell carcinoma of the bladder, is differentially regulated by PPAR in urothelial cancer cells. Int J Cancer. 2009;124:1820–8.
45. Lu Y, Xu Y, Jin F, Wu Q, Shi J, Liu J. Icariin is a PPARα activator inducing lipid metabolic gene expression in mice. Molecules. 2014;19:18179–91.
46. Niu Y, Zhao X, Wu YS, et al. N6-methyl-adenosine (m6A) in RNA: an old modification with a novel epigenetic function. GenomicsProteomics Bioinformatics. 2013;11:8–17.
47. Yu J, Li Y, Wang T, Zhong X. Modification of N6-methyladenosine RNA methylation on heat shock protein expression. Plos One. 2018;13:e198604.
48. Li M, Zhao X, Wang W, et al. Ythdf2-mediated m6A mRNA clearance modulates neural development in mice. Genome Biol. 2018;19:69.
49. Zhong X, Yu J, Frazier K, Weng X, Li Y, Cham CM, Dolan K, Zhu X, Hubert N, Tao Y, et al. Circadian Clock Regulation of Hepatic Lipid Metabolism by Modulation of m6A mRNA Methylation. Cell Rep. 2018;25:1816–28.e1814.
50. Kang H, Zhang Z, Yu L, et al. FTO reduces mitochondria and promotes hepatic fat accumulation through RNA demethylation. J Cell Biochem. 2018;119:5676–85.
51. Gan Z, Wei W, Wu J, et al. Resveratrol and Curcumin Improve Intestinal Mucosal Integrity and Decrease m6A RNA Methylation in the Intestine of Weaning Piglets. ACS omega. 2019;4:17438–46.

Figures

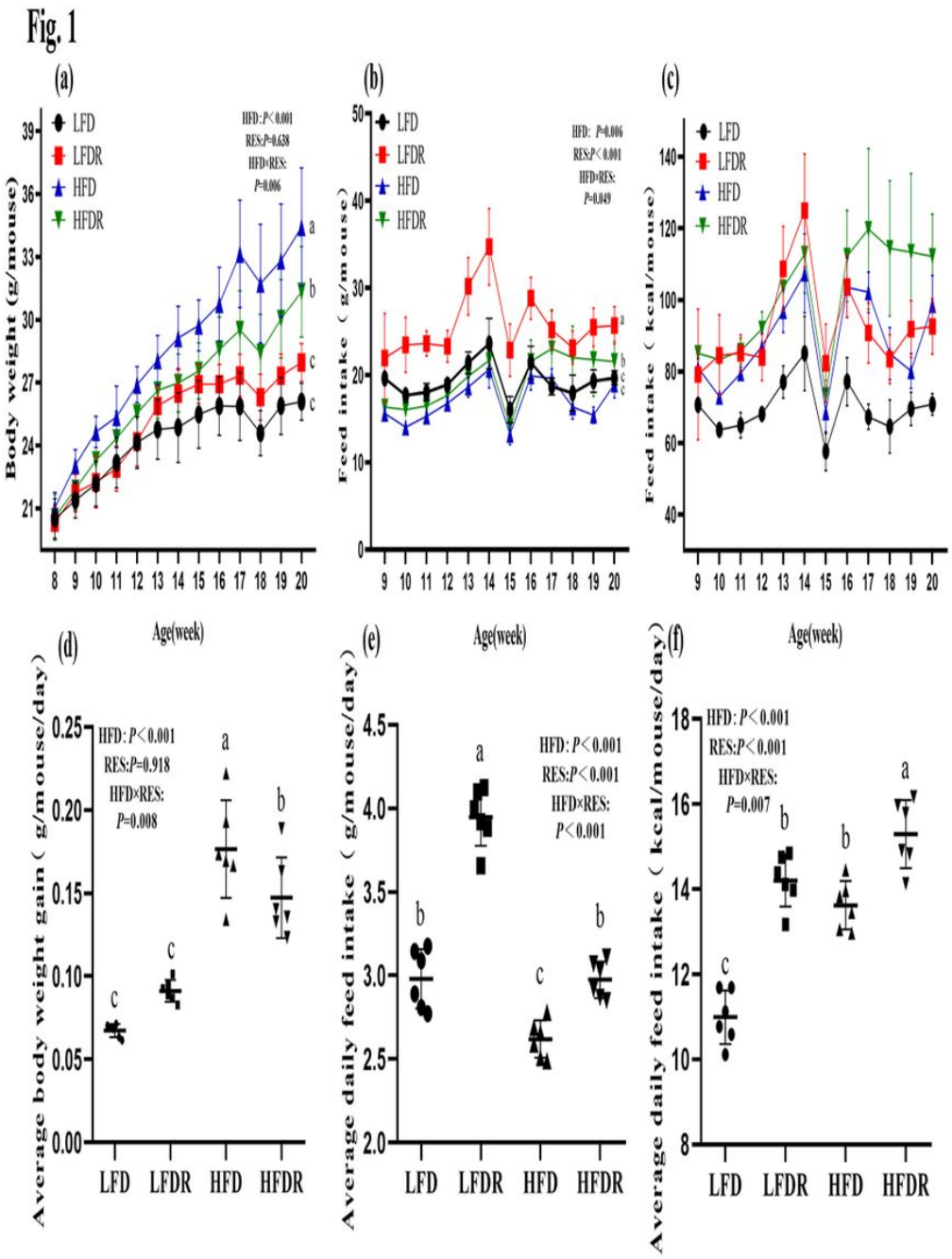

Figure 1

Effect of resveratrol on body weight gain and feed intake. The body weight (a) and feed intake (b) (c) were recorded every week, respectively. Average daily gain (d) and average daily feed intake (e) (f) were calculated. a-c Different or the same superscript letters demonstrate statistically significant differences ($P < 0.05$) and no differences ($P > 0.05$) in groups, respectively (n = 6). LFD, LFDR, HFD, and HFDR represent low-fat, low-fat + 0.0276% resveratrol, high-fat, and high-fat + 0.04% resveratrol, respectively

Fig. 2

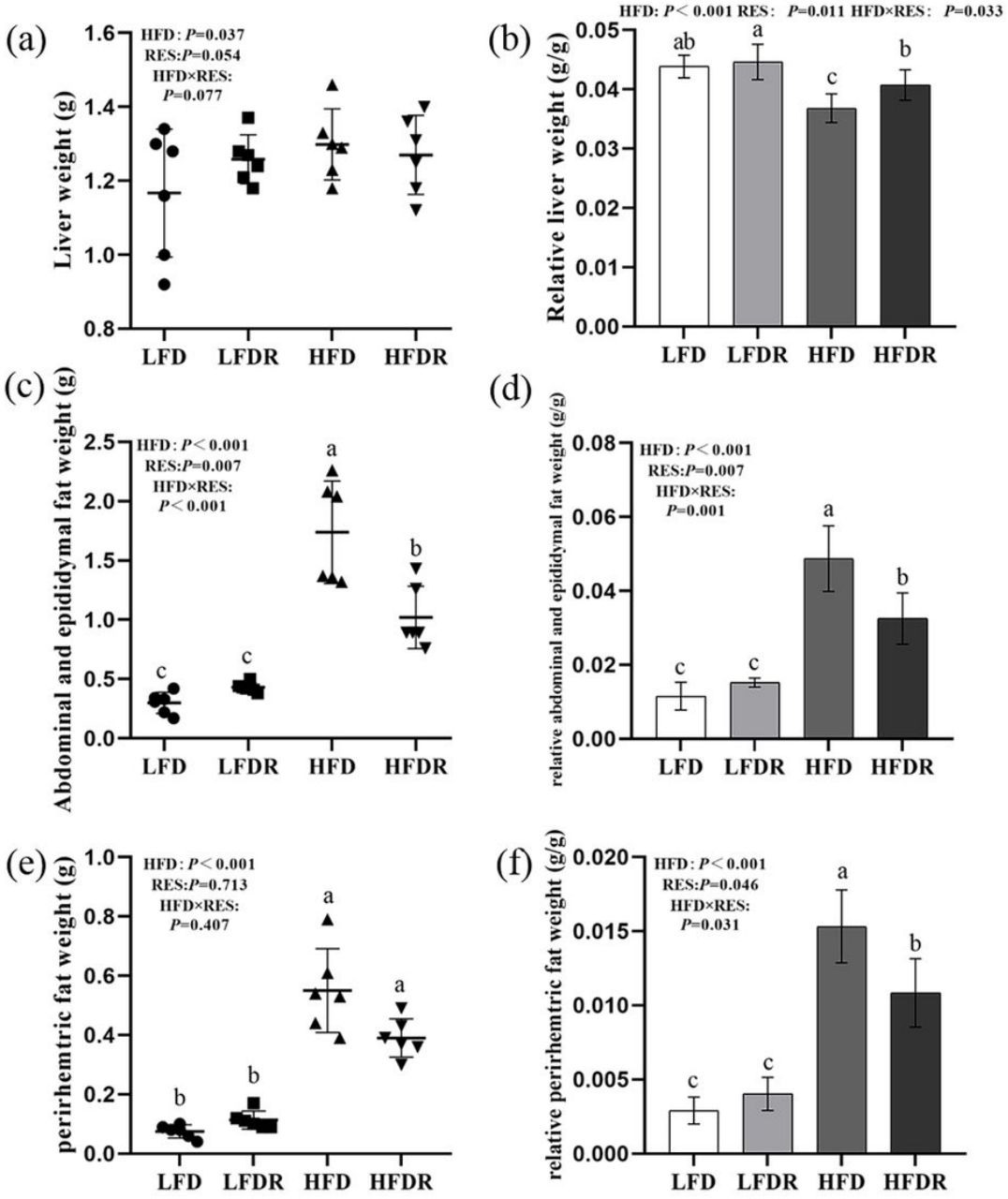

Figure 2

Effect of resveratrol on liver weight gain and fat mass. (a) liver weight; (b) relative liver weight; (c) abdominal and epididymal fat weight; (d) relative abdominal and epididymal fat weight; (e) perirhemtric fat weight; (f) relative perirhemtric fat weight. a-c Different or the same superscript letters demonstrate statistically significant differences ($P < 0.05$) and no differences ($P > 0.05$) in groups, respectively (n = 6). LFD, LFDR, HFD, and HFDR represent low-fat, low-fat + 0.0276% resveratrol, high-fat, and high-fat + 0.04% resveratrol, respectively.

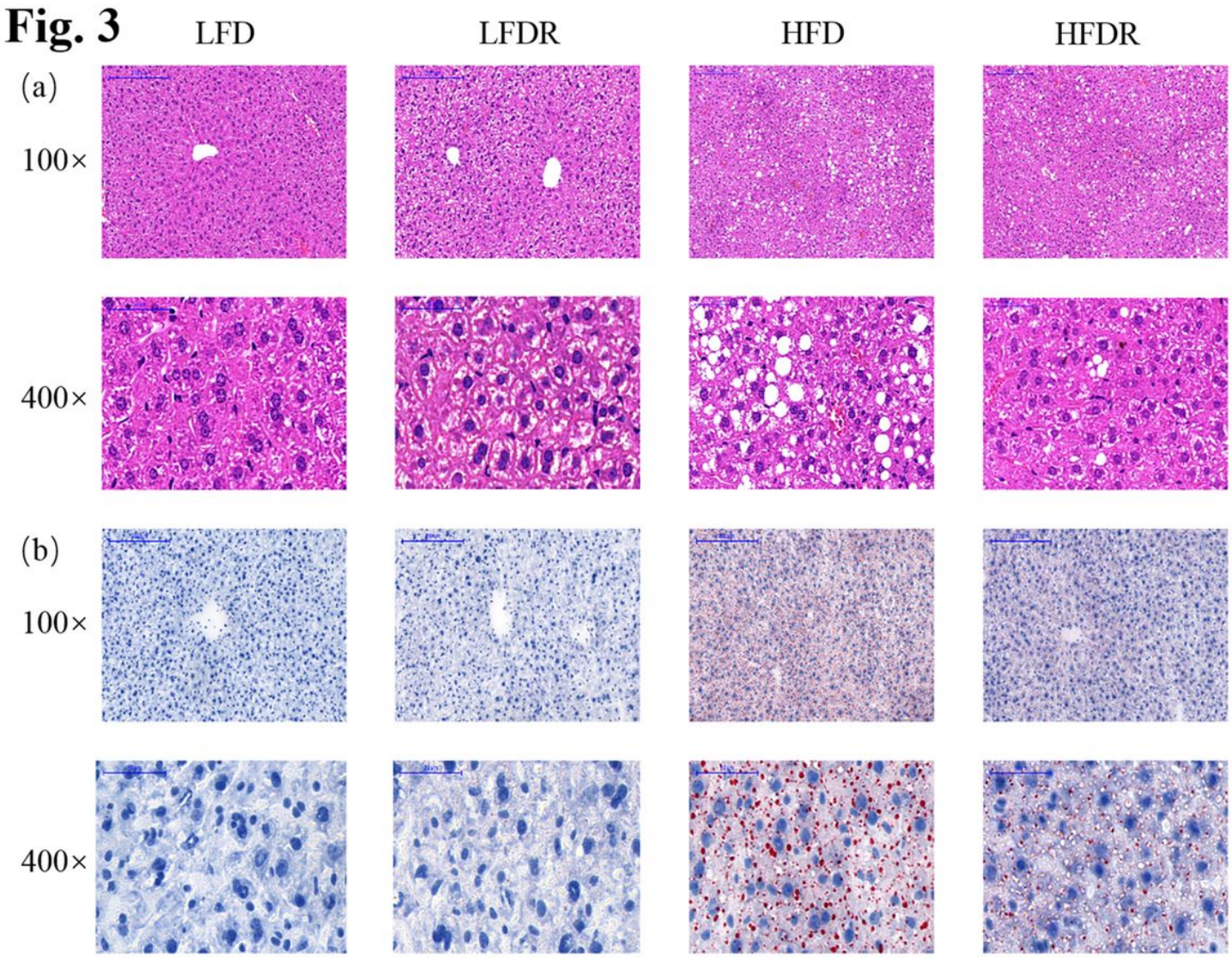

Figure 3

Effect of resveratrol on hepatic lipid droplets in mice. (a) hematoxylin-eosin staining in the liver; (b) Oil-red O staining in the liver. Scale bar (100X) = 200μm; scale bar (400X) = 50μm. LFD, LFDR, HFD, and HFDR represent low-fat, low-fat + 0.0276% resveratrol, high-fat, and high-fat + 0.04% resveratrol, respectively.

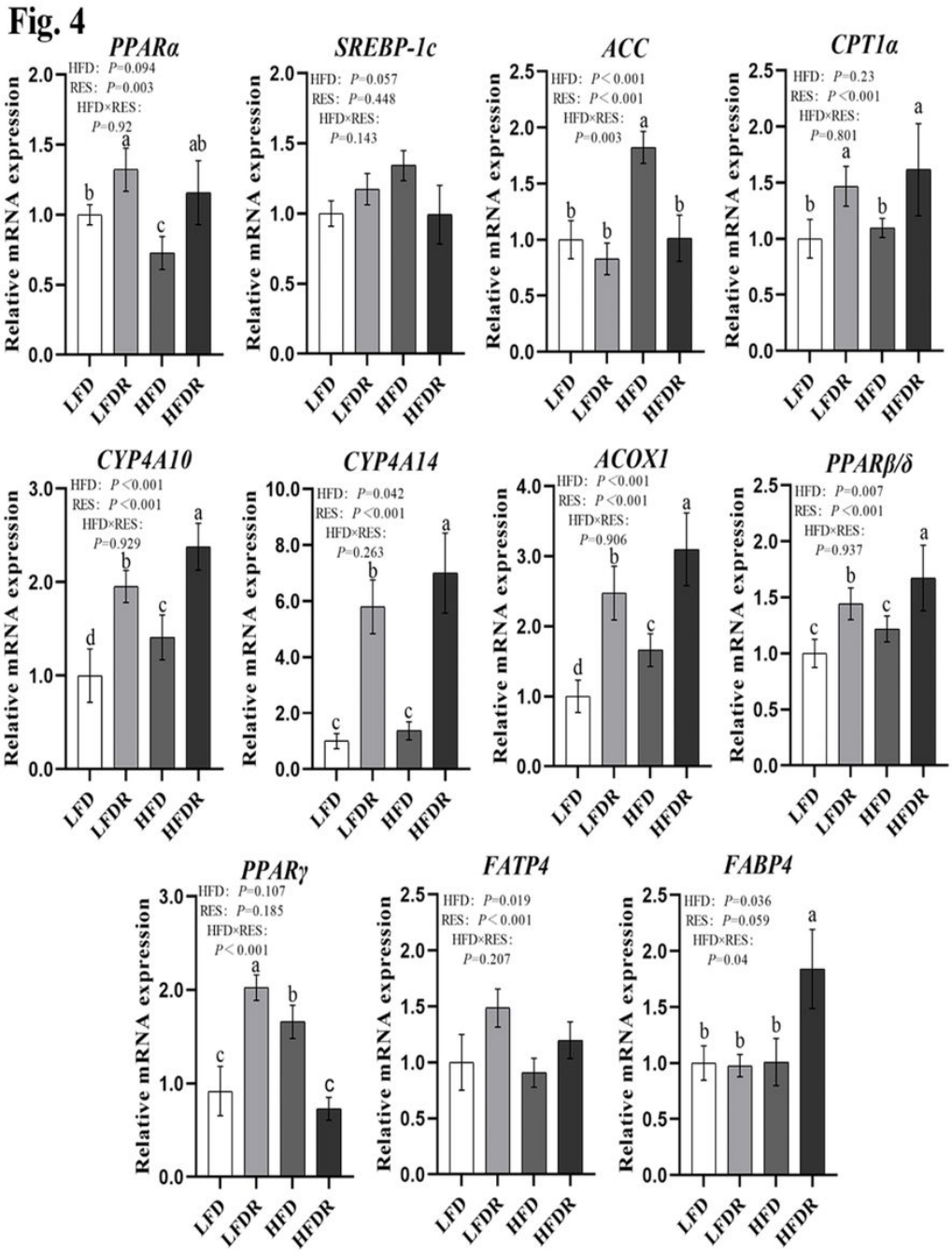

Figure 4

Effect of resveratrol on hepatic lipid metabolism-related genes expression in mice. a-d Different or the same superscript letters demonstrate statistically significant differences ($P < 0.05$) and no differences ($P > 0.05$) in groups, respectively (n = 6). LFD, LFDR, HFD, and HFDR represent low-fat, low-fat + 0.0276% resveratrol, high-fat, and high-fat + 0.04% resveratrol, respectively.

Fig. 5

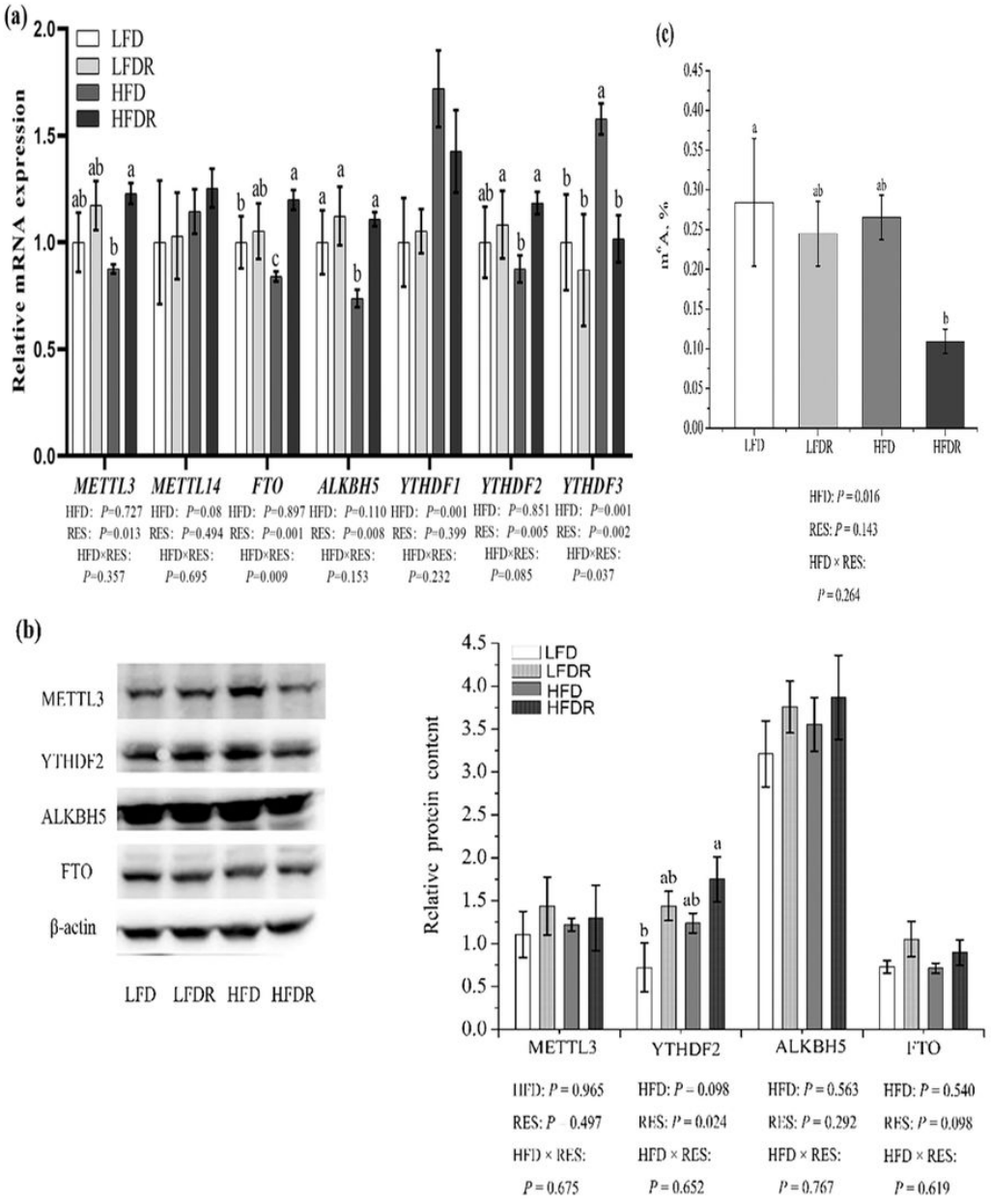

Figure 5

Effect of resveratrol on m6A RNA methylation in the liver. (a) m6A RNA methylation-related genes levels (METTL3, METTL14, FTO, ALKBH5, YTHDF1, YTHDF2, and YTHDF3); (b) m6A RNA methylation-related protein levels (METTL3, YTHDF2, ALKBH5 and FTO) (c) the content of m6A. a-c Different or the same superscript letters demonstrate statistically significant differences ($P < 0.05$) and no differences ($P > 0.05$) in groups, respectively ($n = 6$). (METTL3, 65-70kDa; FTO, 58kDa; ALKBH5, 40-50kDa; YTHDF2, 62kDa; β-actin, 42kDa). LFD, LFDR, HFD, and HFDR represent low-fat, low-fat + 0.0276% resveratrol, high-fat, and high-fat + 0.04% resveratrol, respectively.